Compatibility of the Vinylidene Ligand and Perfluorophenoxide

Samantha D. Drouin, Heather M. Foucault, Glenn P. A. Yap, and Deryn E. Fogg*

Center for Catalysis Research and Innovation, Department of Chemistry, University of Ottawa, 10 Marie Curie, Ottawa, Ontario, Canada, K1N 6N5

Received October 28, 2003

This study demonstrates the stability of the Ru-vinylidene moiety toward installation of a perfluorophenoxide ligand. The room-temperature reaction of $RuCl(dcypb)(\mu\text{-}Cl)_3Ru(dcypb)(N_2)$ (**3**) with $TlOC_6F_5$ and excess *tert*-butylacetylene yields mononuclear $Ru(OC_6F_5)_2(dcypb)(=C=CHBu^t)$ (**6**, dcypb = 1,4-bis(dicyclohexylphosphino)butane). Intermediates en route to **6** are the face-bridged dimers $RuCl(dcypb)(\mu\text{-}Cl)_3Ru(dcypb)(=C=CHBu^t)$ (**4a**) and $[\{Ru(dcypb)(=C=CHBu^t)\}_2(\mu\text{-}Cl)_3]OC_6F_5$ (**5**·OC_6F_5): the cation in the latter was characterized as its PF_6 salt (reaction halting at **5**·PF_6 on use of $TlPF_6$ in place of $TlOC_6F_5$). Edge-bridged, dicationic $[\{RuCl(dcypb)(=C=CHBu^t)\}_2(\mu\text{-}Cl)_2](OC_6F_5)_2$ (**8**) is also a probable intermediate in this reaction pathway: although not observed directly, the dication was isolated in low yields as its $BAr^f{}_4$ salt, on reaction of **5**·PF_6 with $NaBAr^f{}_4$ ($BAr^f{}_4{}^- = [B\{C_6H_3(CF_3)_2\text{-}3,5\}_4]^-$). A minor byproduct in the synthesis of **6** is acetylide $Tl[\{Ru(C\equiv CBu^t)(dcypb)\}_2(\mu\text{-}Cl)_3]$ (**7**), formed by deprotonation of the vinylidene ligand in **5**·OC_6F_5 by $TlOC_6F_5$. (An alternative representation of **7** as a covalent $Ru(\mu\text{-}Cl)_2Tl$ species is supported by X-ray evidence, at least in the solid state.) Importantly, the deprotonation reaction is reversible, and competing reprotonation of **7** by the phenol coproduct enables re-formation of **5**·OC_6F_5. Nucleophilic attack by the aryloxide anion on the metal center enables complete and irreversible transformation to **6**, illustrating the mutual compatibility of the vinylidene and perfluorophenoxide ligands. As expected from the high thermodynamic stability of the $Ru_2(\mu\text{-}Cl)_3$ entity, complexes **5**·PF_6 and **5**·Cl exhibit low activity in ring-opening metathesis polymerization of norbornene. Mononuclear **6**, containing four nonlabile ligands cis to the vinylidene moiety, is likewise quite unreactive until activated by protonolysis of aryloxide. Product identities were established by ^1H, ^{13}C, and ^{31}P NMR and IR spectroscopy, and (**6**, **7**, **8**) X-ray crystallography.

Introduction

Olefin metathesis by robust, functional-group-tolerant ruthenium complexes (**1a**/**b**, Chart 1; IMes = *N*,*N*′-bis(mesityl)imidazol-2-ylidene) is a powerful tool in synthetic organic chemistry.[1] The simple chloride ligands prevalent in the Ru chemistry, however, offer limited steric definition of the active site and can facilitate bimolecular deactivation to metathesis-inactive $Ru_2(\mu\text{-}Cl)_3$ dimers.[2] "Pseudohalide" ligands thus hold considerable promise for design of novel catalysts with expanded selectivity and lifetimes. We recently reported the first highly active Ru-alkylidene catalysts containing pseudohalide ligands: in these complexes, the chloride ligands of **1b** are replaced by aryloxide groups.[3] Catalyst **2** displayed high activity at very low catalyst concentrations, achieving turnovers of up to 40 000 in ring-closing metathesis of the benchmark substrate diethyl diallylmalonate.

Chart 1

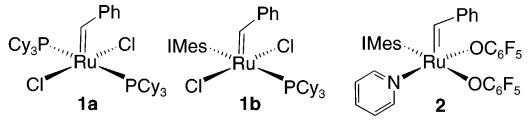

The enhanced robustness and ease of synthesis of vinylidene derivatives,[4] versus alkylidene, prompted our interest in related Ru-vinylidene species. Such catalysts promote a range of transformations, including nucleophilic addition to alkynes, alkyne coupling, cycloaromatization, and olefin metathesis.[4] The vinylidene ligand is susceptible, however, to deprotonation by alkoxides and aryloxides[4] and can also undergo intramolecular attack by carboxylates,[5,6] alcohols,[7] and amides,[8a] although examples are also known in which vinylidene ligands are unperturbed by introduction of anionic

* Corresponding author. E-mail: dfogg@science.uottawa.ca. Fax: (613) 562-5170.

(1) Recent reviews: (a) Trnka, T. M.; Grubbs, R. H. *Acc. Chem. Res.* **2001**, *34*, 18. (b) Fürstner, A. *Angew. Chem., Int. Ed.* **2000**, *39*, 3012. (c) Buchmeiser, M. R. *Chem. Rev.* **2000**, *100*, 1565.

(2) (a) Amoroso, D.; Yap, G. P. A.; Fogg, D. E. *Organometallics* **2002**, *21*, 3335. (b) Amoroso, D.; Snelgrove, J. L.; Conrad, J. C.; Drouin, S. D.; Yap, G. P. A.; Fogg, D. E. *Adv. Synth. Catal.* **2002**, *344*, 757.

(3) Conrad, J. C.; Amoroso, D.; Czechura, P.; Yap, G. P. A.; Fogg, D. E. *Organometallics* **2003**, *22*, 3634.

(4) (a) Bruneau, C.; Dixneuf, P. H. *Acc. Chem. Res.* **1999**, *32*, 311. (b) Bruce, M. I. *Chem. Rev.* **1991**, *91*, 197.

(5) Sanford, M. S.; Valdez, M. R.; Grubbs, R. H. *Organometallics* **2001**, *20*, 5455.

10.1021/om030646a CCC: $27.50
Publication on Web 04/21/2004

Scheme 1. Vinylidene (4a), Allenylidene (4b), or Alkylidene (4c) Ligands Are Obtained, Depending on the Nature of the Alkyne Substituent

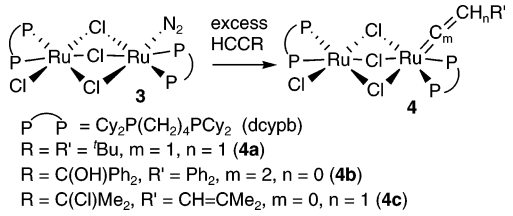

O−O[8b] or N−O[9,10] chelates. In view of this behavior, we wished to evaluate the compatibility of the vinylidene ligand with an electron-deficient aryloxide, in which both basicity and nucleophilicity are much attenuated. With the intention of restricting reactivity to the aryloxide and vinylidene ligands, we chose to explore this chemistry with complexes containing a bulky, nonlabile chelating diphosphine. Dinitrogen-stabilized dimer **3**[11] provides a convenient entry point into dcypb-cumulenylidene complexes, via reaction with terminal alkynes (Scheme 1).[2a,4] We find that a range of dinuclear and mononuclear vinylidene complexes is accessible on reaction of **3** with $TlOC_6F_5$ and alkyne, in which perfluorophenoxide functions as counterion *or* as ligand. No evidence for attack of aryloxide on C_α is found. Deprotonation of C_β is observed, but this reversible reaction does not hamper coordination of aryloxide to the metal to effect quantitative transformation into a stable Ru(σ-OAr) vinylidene complex.

Results and Discussion

We earlier noted that the room-temperature reaction of **3** with *tert*-butylacetylene afforded monovinylidene **4a** as the sole product, even where the alkyne was employed in excess (Scheme 1).[2a] We now find that addition of $TlOC_6F_5$ *prior* to *tert*-butylacetylene permits quantitative transformation of orange **3** into green **6** within 19 h (~80% isolated yield; Scheme 2, route A). Reversing this order of addition results in very slow formation of **6** (19 days, 22 °C; Scheme 2, route B). We attribute the slow rate of the latter reaction to the exceptional stability of face-bridged intermediate **5**·OC_6F_5 (identified by spectroscopic comparison to the isolable PF_6 salt). Complex **5**·OC_6F_5 is the major component after 22 h, accompanied by **6** and acetylide **7** (ratio 6:3:1). Minor amounts of the acetylide complex were fortuitously isolated from reactions employing 2 equiv of $TlOC_6F_5$, as discussed below. On use of $TlPF_6$ in place of $TlOC_6F_5$ (eq 1), reaction is arrested at the stage of **5**·PF_6 (70% isolated yield; quantitative by NMR). Use of excess $TlPF_6$ does not promote further chloride abstraction.

Scheme 2

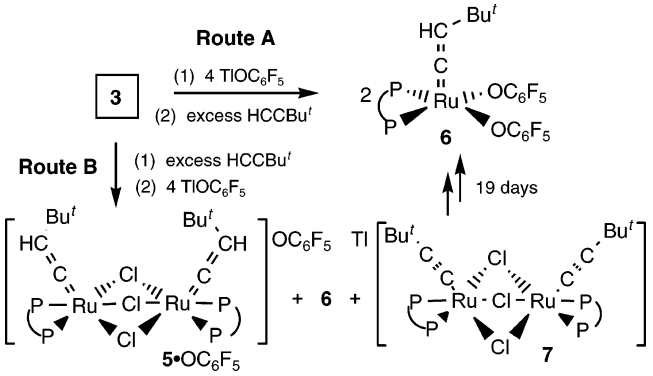

$$\boxed{3} \xrightarrow[\text{(2) excess } TlPF_6]{\text{(1) excess } \equiv\!-Bu^t} \mathbf{5}\cdot PF_6 \qquad (1)$$

The identities of **5**−**7** are supported by spectroscopic data, by X-ray analysis (vide infra) for **6** and **7**, and by microanalytical data for **5** and **6**. The vinylidene ligand gives rise to a strong IR ν(=C=C) band at 1637 cm^{-1} and a characteristically low-field NMR triplet for C_α at 356.8 or 334.9 ppm for **5** or **6**, respectively. The vinylidene proton is observed as a ^1H NMR triplet (**5**, δ_H 3.37; **6**, 3.57 ppm; $^4J_{HP} \approx 3$ Hz), which collapses to a singlet following ^{31}P-decoupling. A sharp singlet due to the *tert*-butyl protons (ca. 1.3 ppm) is visible above the broad, unresolved peaks for the aliphatic dcypb protons. Complexes **5**·OC_6F_5 and **5**·PF_6 are spectroscopically identical, neglecting counterion resonances. $^{31}P\{^1H\}$ NMR analysis of **5**·PF_6 shows, in addition to the high-field PF_6 septet at −144.1 ppm ($^1J_{PF} = 705$ Hz), a single AB quartet (44.3, 43.2; $^2J_{PP} = 26$ Hz). A symmetry plane thus relates the two halves of the cation, but not the two ^{31}P nuclei within a given diphosphine ligand.[12] A similar pattern was reported for $[Ru_2(\mu\text{-}Cl)_3(PPh_3)_4(=C=C=CAr_2)_2]PF_6$.[13] For **6**, the sole ^{31}P NMR resonance is a singlet at 50.0 ppm, consistent with disposition of the two equivalent phosphine ligands trans to perfluorophenoxide. In contrast to the vinylidene complexes, acetylide **7** exhibits a sharp IR band at 2044 cm^{-1} for the ν(C≡C) stretching vibration, and C_α is shifted ca. 200 ppm upfield, to 129 ppm. The location of the *tert*-butyl singlet in the ^1H NMR spectrum is comparatively little affected (δ_H 1.41). A ^{31}P NMR singlet appears at 56.0 ppm.

Acetylide **7** is likely formed in an equilibrium with cationic **5** (Scheme 3) enabled by the capacity of perfluorophenoxide anion to function as a Bronsted, as well as a Lewis, base. Thus, deprotonation of the vinylidene ligands initially competes with nucleophilic attack at the metal. Formation of acetylides by deprotonation at C_β is well established for both cationic and neutral Ru-vinylidene complexes;[14] a recent example involves reaction of NEt_3 with *t*-$[RuCl(dppe)_2(=C=CHMe)]PF_6$.[14a]

(6) (a) A superficially related example almost certainly involves attack of carboxylate on a carbyne species generated in situ by protonation of a Ru-vinylidene. See: González-Herrero, P.; Weberndörfer, B.; Ilg, K.; Wolf, J.; Werner, H. *Organometallics* **2001**, *20*, 3672. (b) González-Herrero, P.; Weberndörfer, B.; Ilg, K.; Wolf, J.; Werner, H. *Angew. Chem., Int. Ed.* **2000**, *39*, 3266.

(7) Rüba, E.; Gemel, C.; Slugovc, C.; Mereiter, K.; Schmid, R.; Kirchner, K. *Organometallics* **1999**, *18*, 2275.

(8) (a) Slugovc, C.; Mereiter, K.; Schmid, R.; Kirchner, K. *Organometallics* **1998**, *17*, 827. (b) Slugovc, C.; Gemel, C.; Shen, J. Y.; Doberer, D.; Schmid, R.; Kirchner, K.; Mereiter, K. *Monatsh. Chem.* **1999**, *130*, 363.

(9) Opstal, T.; Verpoort, F. *J. Mol. Catal. A* **2003**, *200*, 49.

(10) Opstal, T.; Verpoort, F. *Synlett.* **2002**, 935.

(11) Amoroso, D.; Yap, G. P. A.; Fogg, D. E. *Can. J. Chem.* **2001**, *79*, 958.

(12) NMR analysis does not distinguish between the cisoid and transoid isomers, though the former is represented in Scheme 2 by analogy with the crystallographically determined structure for **7**: in principle a ^{31}P NMR singlet would be expected for either structure.

(13) Touchard, D.; Guesmi, S.; Bouchaib, M.; Haquette, P.; Daridor, A.; Dixneuf, P. H. *Organometallics* **1996**, *15*, 2579.

Scheme 3

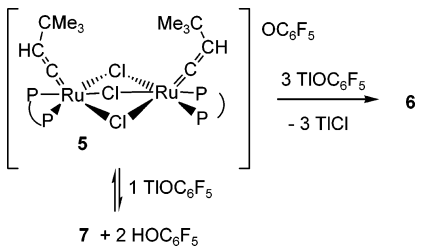

Such reactions have been proposed as an essential activating step in catalytic coupling[15] and stoichiometric hydration[16] of terminal alkynes. Limiting the yields of **7** in the present case (and ultimately permitting complete formation of **6**) is reprotonation of the acetylide ligand by the acidic perfluorophenol coproduct (pK_a 5.5).[17] Independent reaction of isolated **7** with 10 equiv of HOC_6F_5 indeed effects complete transformation into **5**·OC_6F_5, within 10 min at RT (^{31}P NMR).[18] These observations prompted us to attempt synthesis of **7** via treatment of **5**·PF_6 with TlOEt, which generates the much weaker conjugate acid ethanol (pK_a 18). Isolated yields of **7** were improved to 40%, although some decomposition was also evident by NMR analysis: this could not be separated by reprecipitation, impeding microanalysis.

Efforts to prepare RuCl(OAr)(dcypb)(=C=CH^{t}Bu), containing *one* aryloxide per Ru, by protonolysis of **6** with 1 equiv of HCl, were frustrated by disproportionation to **5**·Cl. Addition of a second equivalent of HCl completed transformation to **5**·Cl (eq 2).[19] We have noted in related work the tendency toward disproportionation with aryloxide nucleophiles, yielding bis(aryloxide) products.[20] No evidence was seen in this chemistry of protonation of the vinylidene to form a cationic carbyne, or of nucleophilic attack on the vinylidene ligand by the oxygen donor of either the aryloxide anion or the neutral phenol,[4−6,21] consistent with the attenuated basicity and nucleophilicity of the OC_6F_5 entity.

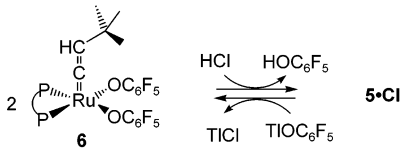

(2)

In contrast with the experiments involving **5** and 2 equiv of aryloxide, the corresponding reaction of **5**·PF_6 with $NaBAr^f_4$ ($BAr^f_4{}^- = [B\{C_6H_3(CF_3)_2\text{-}3,5\}_4]^-$) permits abstraction of one bridging chloride and isolation of edge-bridged dimer **8** (eq 3). Only 20% conversion to **8** is observed after 20 h (^{31}P NMR; 52.4 ppm). While the proportion of **8** increases slightly over a further 24 h in solution, to a maximum of 30%, residual **5**·PF_6 is still present, and significant decomposition is inferred from the presence of multiple peaks from 45 to 47 ppm (50% of total integrated intensity). The identity of **8** was established by X-ray analysis (vide infra) of crystals that deposited from solution over 6 days: the crystallographic observation of two cis-disposed, equivalent phosphine ligands is consistent with the presence of a ^{31}P NMR singlet in the NMR spectrum of the crude reaction mixture. The crystals could not be redissolved, hampering attempts to purify **8** by reprecipitation. IR analysis of the crude product shows a new =C=C stretching band at 1610 cm^{-1} accompanying that for the starting material. In the ^{1}H NMR spectrum, the vinylidene proton for **8** appears as a broad triplet at 4.13 ppm ($^4J_{HP}$ = 3 Hz), downfield of the characteristic triplet for **5**·PF_6 at 3.37 ppm.

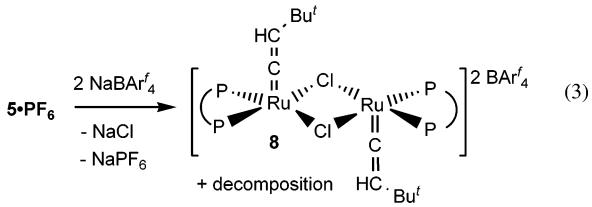

(3)

The stability of the $Ru_2(\mu\text{-}Cl)_3$ unit is highlighted by experiments directed at displacing the vinylidene groups with CO. Treatment of **5**·Cl with CO in refluxing chlorobenzene afforded known [{Ru(dcypb)(CO)}$_2(\mu$-Cl)$_3$]-Cl (**9**)[22,23] and $RuCl_2$(dcypb)(CO)$_2$ (**10**)[11] as major products after 48 h (eq 4). Facile displacement of vinylidene by CO has been reported for several complexes, including RuCl(PNP){=C(NHPh)(CH_2Ph)}(=C=CHPh) (PNP = Pr^{n}N($CH_2CH_2PPh_2$)$_2$),[24] RuCl{HB(pz)$_3$}(PPh_3)(=C=CHPh) (pz = pyrazolyl),[25] [$RuCl_2$(TPPMS)$_2$(=C=CPh$_2$)]-Na_2 (TPPMS = $Ph_2P(o\text{-}C_6H_4OSO_2^-)$),[26] and [RuCl($\kappa^2$-P,O-Pr$^i{}_2PCH_2CH_2$OMe)$_2$(=C=CHPh)]OTf.[27] We presume that carbonylation of **5** occurs via an edge-bridged intermediate of type **8**. The observation of nearly equal proportions of mono- and dinuclear, carbonylated products implies that re-formation of the face-bridged structure

(14) For representative examples, see ref 4 and: (a) Rigault, S.; Monnier. F.; Mousset, F.; Touchard, D.; Dixneuf, P. H. *Organometallics* **2002**, *21*, 2654. (b) Cadierno, V.; Gamasa, M. P.; Gimeno, J.; Gonzalez-Bernardo, C. *Organometallics* **2001**, *20*, 5177. (c) Bruce, M. I.; Ellis, B. G.; Low, P. J.; Skelton, B. W.; White, A. H. *Organometallics* **2003**, *22*, 3184. (d) Bustelo, E.; Carbo, J. J.; Lledos, A.; Mereiter, K.; Puerta, M. C.; Valerga, P. *J. Am. Chem. Soc.* **2003**, *125*, 3311.

(15) (a) Bianchini, C.; Innocenti, P.; Peruzzini, M.; Romerosa, A.; Zanobini, F. *Organometallics* **1996**, *15*, 272. (b) Tenorio, M. A. J.; Puerta, M. C.; Valerga, P. *Organometallics* **2000**, *19*, 1333.

(16) Bianchini, C.; Casares, J. A.; Peruzzini, M.; Romerosa, A.; Zanobini, F. *J. Am. Chem. Soc.* **1996**, *118*, 4585.

(17) Birchall, J. M.; Haszeldine, R. N. *J. Chem. Soc.* **1959**, 3653.

(18) Observation of 20% **6** after 20 h presumably reflects dehalogenation of **5** by $TlOC_6F_5$ coproduct. Complex **6** is a thermodynamic sink in this reaction manifold, the proportion of which is controlled by the amount of $TlOC_6F_5$ available.

(19) Complexes **5**·Cl and **5**·OC_6F_5 were identified by comparison of their spectroscopic features with those of isolated **5**·PF_6. The dinuclear formulation is supported by electrospray mass spectrometric analysis of **5**·Cl, which revealed a molecular ion peak for the cation at *m*/*z* 1409, with the expected isotope pattern.

(20) Snelgrove, J. L.; Conrad, J. C.; Yap, G. P. A.; Fogg, D. E. *Inorg. Chim. Acta* **2003**, *345*, 268.

(21) Daniel, T.; Mahr, N.; Braun, T.; Werner, H. *Organometallics* **1993**, *12*, 1475.

(22) Spectroscopic data do not distinguish between the face-bridged structure shown in eq 4 and the edge-bridged structure originally suggested (ref 23). Ongoing work in this laboratory reveals, however, that the preferred isomer of this and related dimers is strongly solvent-dependent and that the cationic $Ru_2(\mu\text{-}Cl)_3$ form is favored in chlorocarbon solvents. Drouin, S. D.; Yap, G. P. A.; Fogg, D. E. *Organometallics*, in preparation.

(23) Drouin, S. D.; Amoroso, D.; Yap, G. P. A.; Fogg, D. E. *Organometallics* **2002**, *21*, 1042.

(24) Bianchini, C.; Purches, G.; Zanobini, F.; Peruzzini, M. *Inorg. Chim. Acta* **1998**, *272*, 1.

(25) Slugovc, C.; Sapunov, V. N.; Wiede, P.; Mereiter, K.; Schmid, R.; Kirchner, K. *J. Chem. Soc., Dalton Trans.* **1997**, 4209.

(26) Saoud, M.; Romerosa, A.; Peruzzini, M. *Organometallics* **2000**, *19*, 4005.

(27) Martin, M.; Gevert, O.; Werner, H. *J. Chem. Soc., Dalton Trans.* **1996**, 2275.

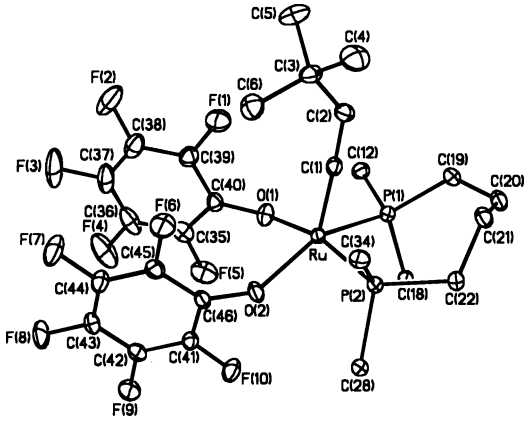

Figure 1. ORTEP diagram for $Ru(OC_6F_5)_2$(dcypb)(=C=CHBu^t), **6**. Thermal ellipsoids are shown at the 30% probability level. For clarity, each cyclohexyl group is abbreviated to a single carbon and hydrogen atoms are omitted.

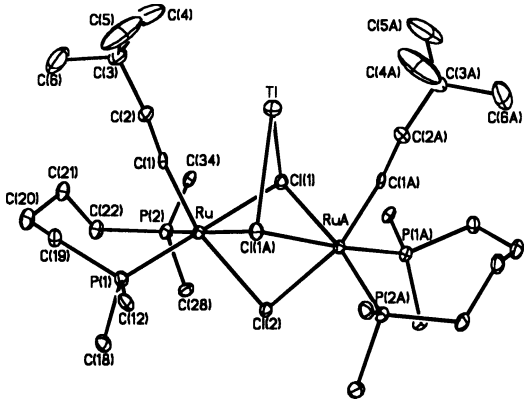

Figure 2. ORTEP diagram of Tl[{Ru(C≡CBu^t)(dcypb)}$_2$-(μ-Cl)$_3$], **7**. Thermal ellipsoids shown at 30% probability level. For clarity, each cyclohexyl group is abbreviated to a single carbon and hydrogen atoms are omitted.

competes with substitution by CO, despite the presence of CO in excess.

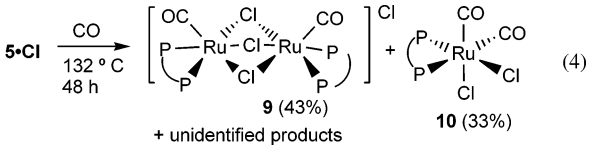

(4)

X-ray Analysis of 6−8. Crystals of **6**, **7**, and **8** suitable for X-ray analysis were grown by slow evaporation of CH_2Cl_2/benzene, benzene, and CH_2Cl_2 solutions, respectively. Their ORTEP diagrams are shown in Figures 1−3, with bond lengths and angles in Tables 1−3. In both mononuclear **6** and dinuclear **8**, the Ru center has approximately square pyramidal geometry, with apical vinylidene. The two metal centers in **8** are related by a C_2 axis, with transoid vinylidene ligands. The P(1)−Ru−P(2) bite angle in **6** (98.45(2)°) is larger than values in bioctahedral complexes of dcypb[28] (for which the value of 92.62(5)° for **7** below is typical), but is comparable to that found in other Ru-dcypb complexes (98.45(2)−100.51(7)°),[23] including **8** (98.76(9)°). The Ru−C(1) bond distances of 1.793(2) Å for **6** and 1.798(4) Å

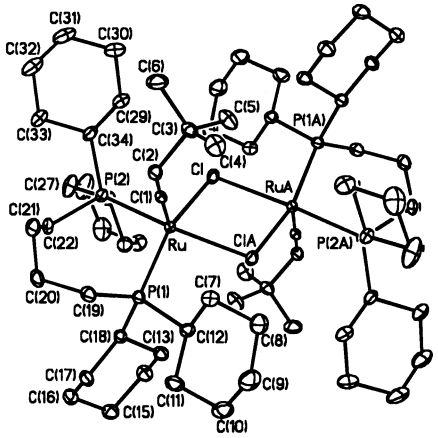

Figure 3. ORTEP diagram of the cationic portion of [{Ru-(dcypb)(=C=CHBu^t)}$_2$(μ-Cl)$_2$](BAr$^f{}_4$)$_2$ **8**. Thermal ellipsoids shown at 30% probability level. For clarity, hydrogen atoms and BAr$^f{}_4$ counterions are omitted.

Table 1. Selected Bond Lengths (Å) and Angles (deg) for $Ru(OC_6F_5)_2$(dcypb)[=C=CH(Bu^t)], 6

Ru−P(1)	2.3309(7)	Ru−O(2)	2.0342(16)
Ru−P(2)	2.3143(6)	C(1)−C(2)	1.316(3)
Ru−C(1)	1.793(2)	O(1)−C(40)	1.305(3)
Ru−O(1)	2.1260(18)	O(2)−C(46)	1.326(3)
P(1)−Ru−P(2)	98.45(2)	C(1)−Ru−P(1)	85.49(7)
O(1)−Ru−O(2)	88.21(7)	C(1)−Ru−P(2)	90.19(8)
O(2)−Ru−P(1)	150.38(6)	C(2)−C(1)−Ru	177.6(2)
O(1)−Ru−P(1)	84.85(5)	Ru−O(1)−C(40)	134.59(17)
O(2)−Ru−P(2)	82.31(5)	Ru−O(2)−C(46)	132.81(15)
O(1)−Ru−P(2)	166.16(6)	C(1)−C(2)−C(3)	130.2(2)

Table 2. Selected Bond Lengths (Å) and Angles (deg) for Tl[{Ru(C≡CBu^t)(dcypb)}$_2$(μ-Cl)$_3$], 7

Ru−C(1)	1.989(5)	Ru−Cl(2)	2.5506(14)
Ru−P(1)	2.2865(14)	Ru−Cl(1A)	2.5459(13)
Ru−P(2)	2.2699(15)	C(1)−C(2)	1.211(7)
Ru−Cl(1)	2.5211(13)	Tl−Cl(1)	2.9157(13)
P(1)−Ru−P(2)	92.62(5)	C(2)−C(1)−Ru	172.9(5)
P(1)−Ru−Cl(1)	175.53(5)	Cl(1)−Ru−Cl(1A)	79.61(5)
P(2)−Ru−Cl(1A)	170.48(5)	Cl(1)−Ru−Cl(2)	78.18(4)
C(1)−Ru−Cl(2)	164.05(14)	Cl(1A)−Ru−Cl(2)	77.73(4)
C(1)−C(2)−C(3)	170.9(6)		

Table 3. Selected Bond Lengths (Å) and Angles (deg) for [{Ru(dcypb)(=C=CHBu^t)}$_2$(μ-Cl)$_2$](BAr$^f{}_4$)$_2$, 8

Ru−C(1)	1.798(4)	Ru−Cl	2.4500(12)
Ru−P(2)	2.3210(12)	Ru−Cl#1	2.5159(11)
Ru−P(1)	2.3594(12)	C(1)−C(2)	1.308(6)
C(1)−Ru−P(2)	89.06(13)	C(1)−Ru−Cl#1	104.01(14)
C(1)−Ru−P(1)	86.98(13)	P(2)−Ru−Cl#1	163.85(4)
P(2)−Ru−P(1)	98.76(4)	P(1)−Ru−Cl#1	91.46(4)
C(1)−Ru−Cl	108.66(13)	C(2)−C(1)−Ru	178.4(4)
P(2)−Ru−Cl	90.70(4)	Cl−Ru−Cl#1	76.28(4)
P(1)−Ru−Cl	161.94(4)	C(1)−C(2)−C(3)	125.7(4)

for **8** are typical for Ru-vinylidenes (cf. values of 1.768-(17) Å in $RuBr_2$(=C=CH^{t}Bu)(PPh_3)$_2$[29] and 1.7903 Å in [RuCl(κ^2-P,O-Pr$^i{}_2$PCH$_2$CH$_2$OMe)$_2$(=C=CHPh)]OTf),[27] as are the C(1)−C(2) bond distances of 1.316(3) Å for **6** and 1.308(6) Å for **8**. The Ru−O bond lengths in **6** (2.1260-(18) and 2.0342(16) Å) are similar to values for aryloxide complexes RuH(OC_6H_4-*p*-Me)(CO)(PMe_3)$_3$ (2.108(6) Å)[30a] and *cis*-RuH(OC_6H_4-*p*-Me)(PMe_3)$_4$ (2.145(6) Å),[30b] as

(28) Amoroso, D.; Haaf, M.; Yap, G. P. A.; West, R.; Fogg, D. E. *Organometallics* **2002**, *21*, 534.

(29) Wakatsuki, Y.; Koga, N.; Yamazaki, H.; Morokuma, K. *J. Am. Chem. Soc.* **1994**, *116*, 8105.

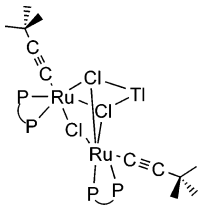

Figure 4. Alternative representation of complex **7** as a covalent, Ru(μ-Cl)$_2$Tl species.

well as those in catalyst **2** (2.076(3), 2.110(3)[3] Å). Both Ru−O bonds in **6** tilt toward the vacant site, and the O atoms are displaced by 14° and 34° out of the sterically congested P−Ru−P plane. Alignment of the two perfluorophenoxide groups deviates by only 9.3° from coplanarity, while the centroid-to-centroid distance of 3.28 Å suggests a π-stacking interaction, by comparison with the interlamellar distance in graphite (3.354 Å).[31] We noted a similar interaction between the two perfluorophenoxide groups in **2**.[3]

Dinuclear **7** is a cofacial bioctahedron, with a C_2 axis through the chloride bridges, such that only half the polyhedron is symmetry-independent. This complex affords a rare example of halide bridges between thallium and transition metals: bonding interactions exist between the thallium "counterion" and two bridging chlorides (Tl−Cl = 2.9157(13) Å), placing the thallium atom equidistant between the Ru centers (Tl−Ru = 3.437(14) Å). The closest intermolecular approach to thallium (4 Å) involves a methylene carbon of a cyclohexyl group. The Tl coordination environment is thus similar to that reported for [Ru(dppe)$_2$(μ_2-F)$_2$](Tl)(PF$_6$).[32] While Scheme 2 shows **7** as the Tl(I) salt, a comparison of the Tl−Cl distance with the sum of ionic radii (3.30 Å) suggests that a covalent representation (Figure 4) is valid, at least in the solid state.

The Ru−C(1) and C(1)−C(2) bond distances (1.989(5) and 1.211(7) Å, respectively) are close to those in Ru(η^5-C$_5$Me$_5$)(C≡CSiMe$_3$)(PPh$_3$)$_2$ (2.004(4) and 1.213(5) Å)[33] and *ttt*-Ru(C≡CSiMe$_3$)$_2$(PEt$_3$)$_2$(CO)$_2$ (2.062(2) and 1.221(2) Å),[34] showing little sensitivity to changes in the ligand environment. The Ru−Ru separation of 3.467(14) Å, similar to that found in [Ru$_2$(μ-Cl)$_3$(PEt$_2$Ph)$_6$]$^+$ (3.443(4) Å),[35] suggests a repulsive rather than an attractive metal−metal interaction.[36] The acetylide ligand is nearly linear, with Ru−C(1)−C(2) and C(1)−C(2)−C(3) bond angles of 172.9(5)° and 170.9(6)°, respectively, the former comparing closely to the Ru−C(1)−C(2) angle of 173.8(4)° in Ru(η^5-C$_5$Me$_5$)(C≡CSiMe$_3$)(PPh$_3$)$_2$.[33]

ROMP via Vinylidene Complexes. Ruthenium vinylidene complexes are attractive targets in the design of novel metathesis catalysts owing to their accessibility and stability; in recent years, numerous Ru-vinylidene metathesis catalysts have been reported,[37] including examples that show activity under aerobic conditions.[37a] Low metathesis activity is anticipated for complexes **5** and **6**, in which the coordination sites cis to the vinylidene ligand are blocked by nonlabile ligands and in which dissociation to coordinatively unsaturated Ru$_1$ species is inhibited by the high stability of the Ru$_2$(μ-Cl)$_3$ moiety. We recently reported that such face-bridged species can function as catalyst sinks in metathesis chemistry,[2a] owing to the high stability of the dimers in noncoordinating solvents. Consistent with this is the performance of **5**·Cl and **5**·PF$_6$ in ROMP of norbornene (NBE): at monomer conversions above 8%, the extremely viscous solutions *resisted even dilution*, suggesting rates of initiation much lower than propagation (Table 4). Dramatically higher initiation rates are found for labile, edge-bridged dimers, which permit access to monouclear active species.[38] In view of the difficulties in isolating edge-bridged **8** noted above, we attempted to generate this species in situ in the presence of norbornene, by treating **5**·PF$_6$ with NaBAr$^f_4$. The rate of formation of **8** is very slow, however (vide supra), and the polymerization profile was thus essentially identical to that observed for catalysis by **5**·PF$_6$.

Table 4. Ru-Catalyzed ROMP of Norbornene (NBE)[a]

entry	catalyst	time (min)	% conv
1	**5**·Cl	40[b]	9[c]
2	**5**·PF$_6$	20[b]	9[c]
3	**6**	1200	44[d]
4	**6**[e]	420[f]	>99
5	**6**[e]	20	23
6	**11a**[g,h]	1440	19
7	**11b**[g]	120	>99

[a] Reaction conditions, unless otherwise noted: CH_2Cl_2 or CD_2Cl_2 solvent, [norbornene]:[Ru] = 100, initial [Ru] = 10 mM, 22 °C; conversions determined by ^{1}H NMR. Low solubility for isolated polymers precluded GPC analysis. [b] Extreme viscosity prevents stirring after this time. [c] Isolated yield. [d] Conversion at 270 min is 11%. [e] Additive: 10 mM [H(OEt$_2$)$_2$]BAr$^f_4$ (control experiments show no ROMP in the absence of Ru over 24 h). [f] Solution diluted with 1 mL/h CH_2Cl_2. [g] Ref 37d. [h] Reaction at 40 °C.

The square pyramidal geometry of **6**, in which the apical vinylidene ligand is cis to four nonlabile phosphine or aryloxide donors, was expected to prevent metathesis until such activity was triggered by (e.g.) protonolyis of an aryloxide group. Such precisely controllable turn-on behavior, which would enable packaging of precatalyst with monomer, is a target property in bulk ROMP applications.[39] Surprisingly, **6** effects ROMP of NBE at 22 °C in the absence of additives, possibly via rate-determining decoordination of one "arm" of the dcypb ligand or isomerization (vide infra). Activity is low, however (20 h for 44% conversion; [NBE]:[Ru] = 100:1), until [H(OEt$_2$)$_2$]BAr$^f_4$ is added, following which polymerization is complete in 7 h.[40]

(30) (a) Hartwig, J. F.; Andersen, R. A.; Bergman, R. G. *Organometallics* **1991**, *10*, 1875. (b) Osakada, K.; Ohshiro, K.; Yamamoto, A. *Organometallics* **1991**, *10*, 404.

(31) Cotton, F. A.; Wilkinson, G. *Advanced Inorganic Chemistry*, 3rd ed.; John Wiley & Sons: Toronto, 1988.

(32) Barthazy, P.; Togni, A.; Mezzetti, A. *Organometallics* **2001**, *20*, 3472.

(33) Kawata, Y.; Sato, M. *Organometallics* **1997**, *16*, 1093.

(34) Sun, Y.; Taylor, N. J.; Carty, A. J. *Organometallics* **1992**, *11*, 4293.

(35) Alcock, N. W.; Raspin, K. A. *J. Chem. Soc., A* **1968**, 2108.

(36) (a) Crozat, M. M.; Watkins, S. F. *J. Chem. Soc., Dalton Trans.* **1972**, 2512. (b) Cotton, F. A.; Ucko, D. A. *Inorg. Chim. Acta* **1972**, *6*, 161. (c) Summerville, R. H.; Hoffmann, R. *J. Am. Chem. Soc.* **1979**, *101*, 3821.

(37) For representative examples, see ref 4a and: (a) Louie, J.; Grubbs, R. H. *Angew. Chem., Int. Ed.* **2001**, *40*, 247. (b) Saoud, M.; Romerosa, A.; Peruzzini, M. *Organometallics* **2000**, *19*, 4005. (c) Schwab, P.; Grubbs, R. H.; Ziller, J. W. *J. Am. Chem. Soc.* **1996**, *118*, 100. (d) Katayama, H.; Ozawa, F. *Chem. Lett.* **1998**, 67. (e) del Rio, I.; van Koten, G. *Tetrahedron Lett.* **1999**, *40*, 1401. (f) Katayama, H.; Yoshida, T.; Ozawa, F. *J. Organomet. Chem.* **1998**, *562*, 203.

(38) Hansen, S. M.; Volland, M. A. O.; Rominger, F.; Eisentrager, F.; Hofmann, P. *Angew. Chem., Int. Ed.* **1999**, *38*, 1273.

(39) Dino Amoroso, Promerus LLC (Brecksville, OH), personal communication.

Periodic dilution was essential for complete reaction (entry 4). In comparison, ROMP via $RuCl_2$(dcypb)(=CHPh) is highly efficient (100% ROMP of 200 equiv of NBE in <2 min at RT): modeling studies suggested the energetic accessibility of an isomer with *basal* alkylidene,[41] precluding the need for phosphine decoordination. It may be noted that the high activity of perfluorophenoxide catalyst **2** is enabled by loss of the labile neutral donor pyridine.[3]

The **6**-$[H(OEt_2)_2]BAr^f{}_4$ system is more active than $RuCl_2(PR_3)_2(=C=CHBu^t)$ (R = Ph, **11a**, entry 6),[37d] attesting to the activating effect of an electron-rich phosphine, but it is considerably less so than **11b** (R = Cy, entry 7). The latter observation may reflect rate limitations associated with retention of two bulky phosphine donors in **6**-$[H(OEt_2)_2]BAr^f{}_4$. Consistent with enhanced steric definition at the active site is the increased cis content of the polynorbornene obtained (25%), relative to that found using **11b** (10%; both at 100% conversion).[37d]

Conclusions

The foregoing illustrates the differing capacity of different halide-abstracting agents to cleave the very stable $Ru_2(\mu\text{-}Cl)_3$ framework of **4a** in the presence of excess *tert*-butylacetylene, affording access to a range of vinylidene products. Isolated are dimeric, face-bridged **5**·PF_6 ($TlPF_6$), edge-bridged **8** ($NaBAr^f{}_4$), or mononuclear **6** ($TlOC_6F_5$), the major product depending also on the coordinating ability of the anion. The vinylidene ligand proves stable against functionalization by perfluorophenoxide. While vinylidene *deprotonation* was observed following reaction of **5**·PF_6 with $TlOC_6F_5$, yielding acetylide **7**, this reaction is reversible, and competing reprotonation of **7** by the phenol coproduct regenerates **5**·OC_6F_5. The low ROMP activity of **5**·PF_6 and **5**·Cl is predicted from our earlier identification of $Ru_2(\mu\text{-}Cl)_3$ species as deactivation products accessible from chlororuthenium metathesis catalysts. Indeed, the limited catalyst lifetimes associated with such deactivation pathways provide a key motivation for development of pseudohalide-containing Ru catalysts such as **2**. Demonstration of the mutual compatibility of perfluorophenoxide and vinylidene functionalities opens the way to synthesis and use of vinylidene catalysts related to **2**, and we are now pursuing routes to such species.

Experimental Section

General Procedures. All reactions were carried out at RT (22 °C) under N_2 using standard Schlenk or drybox techniques, unless stated otherwise. Dry, oxygen-free solvents were obtained using an Anhydrous Engineering solvent purification system and stored over Linde 4 Å molecular sieves. $CDCl_3$, C_6D_6, and toluene-d_8 were dried over activated sieves (Linde 4 Å) and degassed by consecutive freeze/pump/thaw cycles. $RuCl(dcypb)(\mu\text{-}Cl)_3Ru(dcypb)(N_2)$ (**3**) was prepared as previously described.[11] Norbornene was purchased from Aldrich and distilled from sodium under N_2. $[H(OEt_2)_2]BAr^f{}_4$ was prepared by a literature method.[42] Thallium and sodium salts (Strem) and 3,3-dimethyl-1-butyne (Aldrich) were used as received. ^1H NMR (300 or 500 MHz), ^{31}P NMR (121 MHz), and ^{13}C NMR (75 MHz) spectra were recorded on a Bruker Avance-300 or Bruker AMX-500 spectrometer. IR spectra were measured on a Bomem MB100 IR spectrometer. Microanalyses were carried out by Guelph Chemical Laboratories Ltd., Guelph, Ontario.

[{Ru(dcypb)(=C=CHBu^t)}$_2$(μ-Cl)$_3$]PF$_6$ (5·PF$_6$). (a) A suspension of bright orange **3** (120 mg, 0.094 mmol) and 3,3-dimethyl-1-butyne (232 μL, 1.88 mmol) in 5 mL of chlorobenzene was stirred at RT for 18 h, after which time complete conversion to known[2a] **4a** was confirmed by ^{31}P NMR analysis. Addition of $TlPF_6$ (33 mg, 0.094 mmol) effected conversion to **5**·PF_6 over 3 h. The suspension was filtered through neutral alumina, the filtrate was reduced in volume, and hexanes were added to precipitate the pale yellow product, which was recrystallized from toluene and washed with Et_2O and hexanes. Yield: 99 mg (70%). $^{31}P\{^1H\}$ NMR (CD_2Cl_2, δ): 44.4, 43.2 (ABq, $^2J_{PP}$ = 26 Hz), −144.1 (sept, PF_6, $^1J_{PF}$ = 705 Hz). ^1H NMR (CD_2Cl_2, δ): 3.37 (t, 1 H, Ru=C=C*H*, $^4J_{HP}$ = 3.9 Hz), 2.71−1.17 (m, 64 H, Cy and CH_2 of dcypb; Bu^t CH_3), 1.22 (s, Bu^t within Cy envelope). $^{13}C\{^1H\}$ NMR (CD_2Cl_2, δ): 356.8 (t, Ru=*C*, $^2J_{CP}$ = 18.6 Hz), 120.8 (s, RuC=*C*), 40.5−20.6 (aliphatic). IR (Nujol; cm^{-1}): ν(=C=C) 1636. Anal. Calcd for $C_{68}H_{124}Cl_3F_6P_5Ru_2$: C, 53.76; H, 8.23. Found: C, 53.48; H, 8.48. (b) An orange solution of ethereal HCl (150 μL of a 2.0 M solution; 0.30 mmol) and **6** (150 mg, 0.15 mmol) in 3 mL of chlorobenzene was stirred at RT for 2 h, after which $TlPF_6$ (26 mg, 0.074 mmol) was added. After a further 2 h, the suspension was filtered through Celite. Concentration of the filtrate and addition of toluene and hexanes precipitated the yellow product, which was filtered off, washed with Et_2O, and reprecipitated from CH_2Cl_2/hexanes. Yield: 85 mg (76%).

[{Ru(dcypb)(=C=CHBu^t)}$_2$(μ-Cl)$_3$]Cl, 5·Cl. A solution of ethereal HCl (60 μL of a 2.0 M solution, 0.12 mmol) and **6** (60 mg, 0.062 mmol) in 5 mL of CH_2Cl_2 was stirred at RT for 30 min, after which it was concentrated and pentane added. The orange product was filtered off, washed with pentane, and reprecipitated from CH_2Cl_2/pentane. Yield: 33 mg (75%). Spectroscopic data agree with those for **5**·PF_6. ESI-MS: calcd for $C_{68}H_{124}Cl_3P_4Ru_2$ (M^+) 1409, found *m*/*z* 1409.

Ru(OC$_6$F$_5$)$_2$(dcypb)(=C=CHBu^t), 6. (a) A suspension of **3** (344 mg, 0.270 mmol) and $TlOC_6F_5$ (418 mg, 1.08 mmol) in 15 mL of chlorobenzene was stirred at RT for 18 h, over which time it changed color from orange to brown. 3,3-Dimethyl-1-butyne (688 μL, 5.59 mmol) was added and stirring continued for 1 h at RT. The suspension was filtered through Celite. Concentration of the filtrate and addition of hexanes gave **6** as a green powder, which was washed with MeOH and Et_2O and reprecipitated from CH_2Cl_2/hexanes. Yield: 410 mg (78%). X-ray quality crystals were obtained by slow evaporation of a CH_2Cl_2/C_6H_6 solution. $^{31}P\{^1H\}$ NMR (CD_2Cl_2, δ): 50.0 (s). ^1H NMR (CD_2Cl_2, δ): 3.57 (t, 1 H, Ru=C=C*H*, $^4J_{HP}$ = 3.3 Hz), 2.55−1.31(m, 64 H, Cy and CH_2 of dcypb; Bu^t CH_3), 1.33 (s, Bu^t within Cy envelope). $^{13}C\{^1H\}$ NMR (CD_2Cl_2, δ): 334.9 (t, Ru*C*, $^2J_{CP}$ = 21.4 Hz), 142.8 (br s, *ipso-C* of OC_6F_5), 141.3 (d, Ar, $^1J_{CF}$ = 237 Hz), 138.3 (d, Ar, $^1J_{CF}$ = 244 Hz), 130.9 (d, Ar, $^1J_{CF}$ = 236 Hz), 126.0 (s, RuC=*C*), 20−37 (aliphatic). $^{19}F\{^1H\}$ NMR (CD_2Cl_2, δ): −88.10 (m, 2 F), −95.30 (m, 2 F), −106.30 (m, 1 F). IR (Nujol; cm^{-1}): ν(=C=C) 1637. Anal. Calcd for $C_{46}H_{62}F_{10}O_2P_2Ru$: C, 55.25; H, 6.25. Found: C, 55.15; H, 6.50. (b) A suspension of **3** (15 mg, 0.012 mmol) and 3,3-dimethyl-1-butyne (30 μL, 0.24 mmol) in 0.6 mL of chlorobenzene was stirred at RT for 20 h, as above, after which $TlOC_6F_5$ (18.6 mg, 0.048 mmol) was added. Stirring was continued and the reaction monitored by ^{31}P NMR spectroscopy. After 22 h, signals for **5**·OC_6F_5 (58%), **6** (31%), and **7** (11%) were evident. Slow conversion to **6** was observed (complete after 19 days).

(40) We speculate that activation occurs via initial protonolysis and dissociation of a perfluorophenoxide ligand. The possibility that protonolysis occurs at phosphorus seems unlikely in view of in situ ^{31}P NMR experiments that show a single new P-containing species (72.6 ppm, s) and no evidence of the protonated dcypb ligand. Consistent with aryloxide protonation is the observation by ^{19}F NMR of broad multiplets for the free phenol at −87.9 and −93.9 ppm.

(41) Amoroso, D.; Fogg, D. E. *Macromolecules* **2000**, *33*, 2815.

(42) Brookhart, M.; Grant, B.; Volpe, A. F. J. *Organometallics* **1992**, *11*, 3920.

Table 5. Crystal Data and Refinement Details for 6, 7, and 8

	6	7	8
formula	$C_{46}H_{62}F_{10}O_2P_2Ru$	$C_{68}H_{122}Cl_3P_4Ru_2Tl$	$C_{132}H_{148}B_2Cl_2F_{48}P_4Ru_2$
fw	999.97	1576.40	3065.04
temperature	203(2) K	203(2) K	203(2) K
wavelength	0.71073 Å	0.71073 Å	0.71073 Å
cryst syst, space group	monoclinic, *P*2(1)/*n*	monoclinic, *C*2/*c*	triclinic, $P\bar{1}$
unit cell dimens	$a = 13.9203(15)$ Å $\alpha = 90°$ $b = 17.5657(19)$ Å $\beta = 91.803(2)°$ $c = 18.877(2)$ Å $\gamma = 90°$	$a = 14.8162(14)$ Å $\alpha = 90°$ $b = 20.2544(19)$ Å $\beta = 97.025(2)°$ $c = 24.548(2)$ Å $\gamma = 90°$	$a = 14.563(2)$ Å $\alpha = 68.003(2)°$ $b = 15.219(3)$ Å $\beta = 76.178(2)°$ $c = 17.602(3)$ Å $\gamma = 86.912(2)°$
volume	4613.5(9) Å^3	7311.4(12) Å^3	3509.7(10) Å^3
Z, calcd density	4, 1.440 Mg/m^3	4, 1.432 Mg/m^3	1, 1.450 Mg/m^3
absorp coeff	0.486 mm^{-1}	2.840 mm^{-1}	0.409 mm^{-1}
F(000)	2072	3240	1564
cryst size	0.20 × 0.20 × 0.10 mm	0.05 × 0.05 × 0.03 mm	0.30 × 0.20 × 0.20 mm
θ range	1.58 to 28.91°	1.67 to 28.99°	1.44 to 28.71°
limiting indices	$-18 \le h \le 18$, $-23 \le k \le 22$, $-18 \le l \le 25$	$-19 \le h \le 19$, $-27 \le k \le 26$, $-30 \le l \le 31$	$-18 \le h \le 18$, $-20 \le k \le 16$, $-22 \le l \le 17$
no. of reflns collected/unique	31 550/10 720	25 223/8711	19 818/14 279
R(int)	0.0287	0.0908	0.0283
max. and min. transmn	1.000000 and 0.860258	0.9196 and 0.8710	0.9226 and 0.8870
no. of data/restraints/params	10 720/0/550	8711/0/353	19 818/14 279
goodness-of-fit on F^2	1.009	1.000	1.017
final *R* indices [$I>2\sigma(I)$][a]	R1 = 0.0353, wR2 = 0.0782	R1 = 0.0572, wR2 = 0.0704	R1 = 0.0642, wR2 = 0.1356
R indices (all data)	R1 = 0.0529, wR2 = 0.0871	R1 = 0.1193, wR2 = 0.0831	R1 = 0.0982, wR2 = 0.1549
largest diff peak and hole	0.929 and −0.565 e·Å^{-3}	1.210 and −1.160 e·Å^{-3}	1.255 and −1.019 e·Å^{-3}

[a] Definition of *R* indices: $R_1 = \sum(F_o - F_c)/\sum(F_o)$; $wR_2 = [\sum[w(F_o^2 - F_c^2)^2] / \sum[w(F_o^2)^2]]^{1/2}$.

Tl[{Ru(C≡CBu^t)(dcypb)}$_2$(μ-Cl)$_3$], 7. (a) Via Deprotonation of 5·PF$_6$. Addition of TlOEt (20 μL, 0.34 mmol) to a stirred solution of **5**·PF$_6$ (90 mg, 0.060 mmol) in 3 mL of toluene gave a bright yellow solution, which was stirred at RT for 2 h and then filtered through Celite and neutral alumina. Concentration of the filtrate and addition of hexanes precipitated the product, which was filtered off, washed with hexanes, and reprecipitated from THF/hexanes to yield 38 mg (39%) of yellow **7** (contaminated, however, by unknown product(s) observed as a broad multiplet at 44.3 ppm in the ^{31}P NMR spectrum; 5−15% integrated intensity). ^{31}P{^{1}H} NMR for **7** (C_6D_6, δ): 56.0 (br s). ^{1}H NMR (C_6D_6 δ): 3.31−1.10 (m, Cy and C*H*$_2$ of dcypb; Bu^t C*H*$_3$), 1.41 (s, Bu^t within Cy envelope). ^{13}C{^{1}H} NMR (THF-d_8, δ): 129.1 (br s, Ru*C*≡CBu^t); (C_6D_6, δ): 66.0 (br s, RuC≡*C*Bu^t). IR (Nujol; cm^{-1}): ν(C≡C) 2044.

(b) Isolated as a Byproduct in Synthesis of 6. A mixture of **3** (100 mg, 0.079 mmol) and TlOC$_6$F$_5$ (61 mg, 0.16 mmol) in 10 mL of CH_2Cl_2 was stirred at RT for 10 min. The solvent was then removed under vacuum, the orange residue redissolved in 25 mL of THF, and 3,3-dimethyl-1-butyne (195 μL, 1.58 mmol) added by syringe. The solution was stirred at RT for 15 h, then filtered through Celite. The filtrate was concentrated, hexanes were added, and the yellow precipitate was filtered off, washed with Et_2O and hexanes, and dried under vacuum. Yield: 20 mg (16%). ^{31}P NMR analysis of the filtrate revealed a mixture of **6** (40%), **5**·Cl (52%), and **7** (8%). X-ray quality crystals were obtained by slow evaporation of a benzene solution of isolated **7**.

Protonation of Acetylide 7 by HOC$_6$F$_5$. Pentafluorophenol (24 mg, 0.13 mmol) was added to a stirred solution of **7** (15.5 mg, 0.010 mmol) in 0.7 mL of benzene. ^{31}P NMR analysis after 10 min revealed complete conversion to **5**·OC$_6$F$_5$. After 20 h, the singlet for **6** (18%) was also present.

Carbonylation of [{Ru(dcypb)(=C=CHBu^t)}$_2$(μ-Cl)$_3$]Cl, 5·Cl. A solution of **5**·Cl (10.6 mg, 7.5 μmol) in chlorobenzene (2 mL) was refluxed under CO (1 atm) for 48 h. ^{31}P NMR showed a mixture of *ccc*-RuCl$_2$(dcypb)(CO)$_2$ (**10**,[11] 33%) and [{Ru(dcypb)(CO)}$_2$(μ-Cl)$_3$]Cl (**9**,[22,23] 43%). ^{31}P{^{1}H} NMR ($CDCl_3$, δ): 50.8 (d, $^2J_{PP}$ = 23 Hz, **9**), 42.5 (d, $^2J_{PP}$ = 23 Hz, **9**), 39.4 (d, $^2J_{PP}$ = 23 Hz, **10**), 17.1 (d, $^2J_{PP}$ = 23 Hz, **10**). Unidentified byproducts (several overlapping peaks at δ_P 20 ppm) account for 23% of the total integrated intensity.

[{Ru(dcypb)(=C=CHBu^t)}$_2$(μ-Cl)$_2$](BAr$^f_4$)$_2$, 8. A solution of **5**·PF$_6$ (15 mg, 10 μmol) in 0.7 mL of CH_2Cl_2 was stirred at RT as NaBAr$^f_4$ (19 mg, 20 μmol) was added. After 20 h, a new ^{31}P NMR singlet was observed at δ_P 52.4, accompanying that for **5** (ratio 1:4). After 44 h, the proportion of **8** reached 30%; after 6 days, no ^{31}P signal could be observed in solution, but dark brown, X-ray quality crystals of **8** had deposited. ^{31}P{^{1}H} NMR (CD_2Cl_2, δ): 52.4 (s, 50% of total integrated intensity), other peaks include **5**·PF$_6$ (44.4, 43.2, ABq), and several unidentified multiplets between 47 and 45 ppm (not present in the spectrum of the crude reaction mixture). ^{1}H NMR (CD_2Cl_2, δ): 7.72 (br s, BAr$^f_4$), 7.57 (br s, BAr$^f_4$), 4.13 (t, 1 H, Ru=C=C*H*, $^4J_{HP}$ = 3 Hz, **8**), 3.37 (t, 1 H, Ru=C=C*H*, $^4J_{HP}$ = 3.9 Hz, **5**·PF$_6$), 1.17−2.85 (br, Cy and C*H*$_2$ of dcypb; Bu^t C*H*$_3$), 1.27 (s, Bu^t within Cy envelope). ^{19}F{^{1}H} NMR (CD_2Cl_2, δ): 12.56 (s, BAr$^f_4$). IR (CH_2Cl_2; cm^{-1}): ν(C=C) 1610 (**8**) and 1638 (**5**·PF$_6$).

General Procedure for Polymerization of Norbornene. A solution of norbornene (65 mg, 0.70 mmol) in 350 μL of CD_2Cl_2 was added to a rapidly stirred solution of **5** or **6** (7.0 μmol of Ru=C) in CD_2Cl_2 (350 μL). The reaction was monitored by ^{1}H NMR. [H(OEt$_2$)$_2$]BAr$^f_4$, if required, was added to the Ru solution prior to addition to monomer (6.9 mg, 7.0 μmol). Catalyst **5**·Cl was generated in situ by addition of HCl (7.0 μmol) to the solution of **6** prior to adding monomer. For ROMP catalyzed by **5**·Cl or **5**·PF$_6$, reactions were continued until high viscosity prevented further stirring (20 min), following which the polymer was precipitated by addition of MeOH, dried, and weighed.

Structural Determination of 6−8. Suitable crystals were selected, mounted on thin glass fibers using paraffin oil, and cooled to 203(2) K. Data were collected on a Bruker AX SMART 1k CCD diffractometer using 0.3° ω-scans at 0°, 90°, and 180° in ϕ; λ 0.71073 Å. Initial unit-cell parameters were determined from 60 data frames collected at different sections of the Ewald

sphere. Semiempirical absorption corrections based on equivalent reflections were applied (SADABS, Bruker AXS, Madison, WI, 2000).

Systematic absences in the diffraction data and unit-cell parameters for **6** were uniquely consistent with the space group $P2(1)/n$. Those for **7** were consistent with $C2/c$ (No. 15) and Cc (No. 9), while no symmetry higher than triclinic was observed in the diffraction data for **8**. For both **7** and **8**, solution in the centrosymmetric space group option yielded chemically reasonable and computationally stable results of refinement. Structures were solved by direct methods, completed with difference Fourier syntheses, and refined with full-matrix least-squares procedures based on F^2. In the case of **7**, the molecule is located at a 2-fold axis; for **8**, the dimeric dication was located at the inversion center. All non-hydrogen atoms were refined with anisotropic displacement parameters. All hydrogen atoms were treated as idealized contributions. All scattering factors are contained in the SHELXTL 6.12 program library.[43] Table 5 compiles the data for the structure determinations.

(43) Sheldrick, G. M. *SHELXTL 6.12*; Bruker AXS: Madison, WI, 2001.

Acknowledgment. This work was supported by the Natural Sciences and Engineering Research Council of Canada, the Canada Foundation for Innovation, the Ontario Innovation Trust, and the Ontario Research and Development Corporation.

Supporting Information Available: NMR spectra for **7** and **8**, and tables of crystal data collection, refinement parameters, atomic coordinates, bond lengths and angles, anisotropic displacement parameters, and hydrogen coordinates for **6**−**8**. This material is available free of charge via the Internet at http://pubs.acs.org.

OM030646A